ISSN 1022 - 2502, E-ISSN 2408- 8528
Dhaka Univ. J. Sci. 72(2): 52-60, 2024 (July) DOI: https://doi.org/10.3329/dujs.v72i2.75471

Efficacy of Capacitive Deionization Flow Cell Fabricated with Carbon Nanomaterial Modified Electrodes

Mohammad Anikur Rahman, Mohy Menul Islam, Muhammed Shah Miran, Md. Abu Bin Hasan Susan and Md. Mominul Islam*

Department of Chemistry, Faculty of Science, University of Dhaka, Dhaka 1000, Bangladesh

(Received: 11 January 2024; Accepted : 25 June 2024)

Abstract

The supply of freshwater is becoming a serious global challenge. Capacitive deionization (CDI) has been recognized as a promising and smart desalination technique to solve it. Carbonaceous materials, due to their non-toxic characteristics, are used for filtration, adsorption, and water deionization. In this study, a newly designed, homemade low CDI system was fabricated, and carbon as electrode material was prepared from waste leather through a one-step activated pyrolysis process. Carbonaceous materials prepared at different temperatures were characterized by Fourier-transform infrared (FT-IR), scanning electron microscopy (SEM), and X-ray diffraction (XRD) techniques. The charge storage capacity of the carbon materials casted on a glassy carbon electrode was evaluated using cyclic voltammetric and galvanostatic charging-discharging techniques. The fabricated CDI system could be successfully used for the study of the removal capacity of NaCl from an aqueous solution. The removal capacity of carbon prepared at 600 °C from leather is 11.58 mgg^{-1}, which is about three times higher than commercial activated carbon at flow rate and applied potential of 23 mL min^{-1} and 1.0 V, respectively.

Keywords: Capacitive deionization, Flow cell, Carbonaceous material, NaCl solution

I. Introduction

The demand for freshwater is principally driven by the need to support agricultural, industrial, and human consumption activities. It is anticipated that there will be a global inadequacy of water in the forthcoming decades. Notwithstanding, a significant dearth of water resources is presently a prevalent issue encountered throughout the year by approximately 500 million individuals[1,2]. As an illustration, populations residing in arid and semi-arid regions typically experience water crises due to the limited availability of brackish groundwater[3]. The present scenario entails formulating a plan to furnish freshwater, which involves innovating novel techniques for desalinating brackish water. Capacitive deionization (CDI), a novel technology adopted for this purpose, involves the adsorption of charged species within the boundaries of the electric double layer (EDL) formed due to the polarization of electrodes through the application of an electric field. The operational principle is based on the iterative electrosorption process for charging and desorption for discharging. Upon reaching electrode saturation, a regeneration process is initiated by short-circuiting or reversing the applied potential in order to regain the capacity of ion sorption of the CDI electrodes[4,5].

Studies on the performance of CDI have primarily employed carbon-based electrodes, owing to their favorable electrochemical and textural characteristics. Carbon materials possess high electrical conductivity, significant specific surface area, and modifiable pore structure to make them suitable for this technique[6]. Various carbon-based materials, including nitrogen-doped graphene[5], carbon nanotubes[7], aerogel[8], and carbide-derived carbon[9], have been explored as potential options for effective electrodes in CDI. Despite their ability to offer a substantial electrosorption capacity, most of these carbons are accompanied by high costs or require intricate syntheses to restrict their extensive practical applications on a large scale[10].

In designing CDI electrodes with low-cost carbon materials, it is crucial to evaluate their effectiveness and consider sustainability factors. These requisites can be fulfilled by producing activated carbons derived from biowastes as carbonaceous precursors[11]. Heteroatom-doped porous carbon is designed and integrated with biowastes, such as cellulose[12], lignin[13], rice husk[14], natural polysaccharides[15], and collagen[16]and is regarded as a renewable resource that do not emit carbon dioxide. By doing so, it would be possible to ensure a regular and plentiful supply of carbon sources containing nitrogen to suggest achievement of minimization of production costs and process waste[17].Waste leather (WL) is a type of bio waste predominantly composed of collagen, a natural polymer material that accounts for over 80% of its composition. Leather exhibits a distinct inherent arrangement and distinctive chemical makeup, characterized by a significant proportion of hetero-atoms (numerous amino acids) and minimal ash. This facilitates its potential application as a promising precursor for CDI electrodes[18].

*Author for correspondence. e-mail: mominul@du.ac.bd

This study aims at developing a homemade CDI flow cell using glassy carbon electrode modified by carbon materials derived from WL. Carbonaceous adsorbents were synthesized through a simple pyrolysis process that involved carbonization of leather. The condition of pyrolysis was optimized through thermogravimetric analyses, and the carbon materials synthesized at different pyrolysis temperatures were characterized with relevant techniques. The charge storage capacity and efficiency of the CDI electrode in removing ions were examined using common electrolytic solutions including NaCl solution, and the capacity of ion removal was compared with the commercial carbon.

II. Experimental

Materials

The leather sample (pickle pelt leather) used for the precursor material was collected from Anjuman Tannery, Hemayetpur, Dhaka, Bangladesh. Other chemicals like absolute ethanol, CH_3CH_2OH (Sigma, Germany), hydrochloric acid, HCl (Sigma, Germany), poly(vinylidene fluoride), PVDF (Sigma, Germany), *N*,*N*-dimethylformamide, DMF (Alfa Aesar, England), dimethylsulfoxide, DMSO (Merck, Germany), activated carbon, AC (Uni-Chem, China), and NaCl (Sigma, Germany) were used. Deionized (DI) water (conductivity: 0.055 μS cm^{-1} at 25.0 °C) from HPLC grade water purification systems (BOECO, BOE 8082060, Germany) was used in all experiments.

Preparation of carbon from WL through pyrolysis

The WL was cleaned, dried, and smashed into tiny bits. The small segments were dried in an electric oven at 100 °C. The dried sample was then placed in a crucible boat and pyrolyzed at 600 °C at a heating rate of 5 °Cmin^{-1} in an N_2 environment in a tube furnace. The temperature was kept at 600 °C for 3 h. A dark, fluffy, and porous carbon materialcalledas untreated waste leather carbon (UCWL) produced after calcination, which was then further grounded[19,20]. A similar procedure was followed to prepare samples at 500, 700, and 800 °C. The carbon materials produced were labeled as UCWL-*x*N, where *x* was the activation temperature, and N was the N_2 atmosphere. These are UCWL5N, UCWL6N, UCWL7N, and UCWL8N prepared at 500, 600, 700, and 800 °C, respectively.

Characterizations

A Hitachi TG/DTA 7200 thermo analyzer was utilized to conduct a thermogravimetric analysis (TGA) under the N_2 atmosphere. The morphology and chemical structure of the materials prepared were investigated using SEM (JSM-7600F, JEOL, USA) and FT-IR spectrometers (Frontier FT-NIR/MIR, Perkin Elmer, USA). The phase analysis and chemical characterizations of the samples were carried out using X-ray diffraction (XRD) with a Philips PW 1724 X-ray generator. The XRD analysis was performed using an XDC-700 Guinier-Hagg focusing camera and strictly monochromatic CuK_α radiation (λ = 1.540598).

Fabrication of electrodes

The glassy carbon (GC) disk (diameter: 0.3 cm) and GC plate electrode (area: 21.25 cm^2) were used to fabricate prepared carbon materials. GC electrodes were modified using 92 wt% materials mixed with 8 wt% PVDF in a solvent of DMSO to form a 500.0 μL mixture. To make a well-dispersed suspension, sonication of the mixture was carried out for about 1 h and the suspension was drop-casted on the surface of GC electrode. Then it was dried overnight at 60°C in an oven. The thus-fabricated modified GC electrodes were used for the electrochemical and CDI analyses.

Electrochemical characterization and determination of charge storage

Electrochemical measurements were conducted using a computer-controlled electrochemical analyzer system (Model: CHI 1140 C, USA) in a single-compartment, three-electrode cell. Electrochemical measurements were carried out in electrolytic solutions of 0.01 M NaCl. The working electrode used was a modified GC electrode. A spiral Pt wire was used as counter electrode and Ag|AgCl,KCl(sat.) was reference electrode. Before CDI application, the electrochemical characterization of the modified electrode was performed by measuring cyclic voltammograms (CVs) at various potential scan rates (υ). Different current densities were employed to record galvanostatic charging-discharging (GCD) curves within the same potential range. The specific capacitances (C_{sp}) were calculated based on the GCD plots using Eq. (1):

$$C_{\mathrm{sp}} = \frac{i\Delta t}{m\Delta V} \quad (1)$$

where i is the current (A), Δt is the discharging time (s), m is the mass of active material (g), ΔV is the potential window (V)[21,22].

CDI studies

The desalination capacity of prepared electrodes was evaluated using a conventionally designed CDI setup, as depicted in Scheme 1. Symmetric UCWL modified GC electrodes were arranged in a stacked configuration with a

Teflon flow cell. The anode and cathode terminals of an adjustable DC power supply (Dazheng, PS-305D, China) were connected to the electrodes using wires. Throughout the experiments, variations in conductivity and concentration were recorded with time, and the relation between conductivity and concentration is given by Eq. (2)

$$C = 0.5109\,K + 6.0449 \quad (2)$$

where C is the concentration of solution (mg/L) and K represents conductivity ($\mu S/cm$)[5]. The electrosorption capacity (Λ) of the modified electrodes was calculated using Eq. (3):

$$\Lambda = \frac{(C_0 - C_t)V}{M} \quad (3)$$

where C_0 and C_t denote the initial and final NaCl concentrations of the deionization process, respectively, V (in L) is the solution volume, while M (in g) denotes the combined mass of the two electrodes. The duration of the deionization stage in a charge-discharge cycle is represented by t (min)[5,23-27]. The configuration and optimization of the flow cell performance of the CDI cell are further described later.

III. Results and Discussion

The development of a CDI flow system requires the design and development of a flow channel, synthesis of active carbon materials for CDI electrodes, and a successful assembling of these for efficient removal of ions from aqueous solution. A homemade flow channel was devised from the Teflon block, and the carbonaceous materials were prepared from WL for fabricating CDI electrodes. Before the application of these materials in CDI experiments, their necessary characterizations regarding elemental forms, morphology, crystallinity, electrochemical behaviors, and charge storage capacity were performed.

Preparation of carbon materials

The morphology, microstates, functionality, and level of doping depend on the pyrolysis temperature and environment. Four carbon materials were prepared from WL by applying different pyrolysis temperatures. TGA was used to investigate the variation in the weight of WL throughout the carbonization process, as depicted in Fig. 1a. The process of carbonization of WL can be categorized into three distinct steps. Step I: the observed reduction in the weight of the sample can be attributed to the removal of water. It is noted the collagen fibers of leather contains strongly bonded water to develop fibril from protein. During step II: a significant decrease in weight of 70 wt% is observed in the TGA curve. This reduction is associated with the elimination of less stable components of WL, and removing bound water from the polysaccharide and collagen polar groups. At step III: the WL forms a stable carbon structure and gradually reduces weight. Following the carbonization process, the WLs experienced a reduction in weight of approximately 80-85%. The approximate yield of carbon materials is within the range of 15 to 20%. The temperature range of 600-800 °C has been reported to be appropriate for forming carbon-based materials[19,27]. Hence, the carbonization of WL was carried out at 500, 600, 700, and 800 °C to form UCWLs.

Characterizations

Fig. 1b shows FT-IR spectra of UCWL synthesized at various activation temperatures. The spectral feature observed at 3434 cm^{-1} can be attributed to the stretching vibrations of either N–H or O–H bonds, or potentially a combination of both, resulting in an overlapping signal. The C–H stretching band was observed at around 2900 cm^{-1}. The spectral band observed at 1622 cm^{-1} indicates stretching of either C=O or C=N. Additionally, the bands observed at 1080 cm^{-1} indicate the stretching vibrations associated with the S=O functional groups[27,28]. The presence of these bands indicates that the materials prepared from WL contain various possible functional groups as well. Carbon materials formed became self-doped with inherent nitrogen and sulfur elements of the amino acids of collagen fiber of WL.

The surface morphology of the carbon prepared from WL was studied via SEM, as typically represented in Fig. 1 (c, d). The presence of two-dimensional sheet-like structures demonstrates the homogeneity and uniformity of the geometrical form of prepared carbon. The UCWL is obviously less porous with a smaller surface area and the pores are randomly distributed[20,29]. The original SEM image of UCWL6N was typically analyzed using ImageJ software to estimate various parameters to define the characteristics of particles further according to ISO 9276-6. The different parameters of UCWL6N particles were determined and compared (Fig. 1e). The particles are porous stone-like since the aspect ratio value (1.458) is more than 1.0. In addition, the estimated solidity parameter of UCWL6N was found to be 0.835. The trends of numbers of particles with the sizes of 10, 50, and 100 nm are similar and equally distributed.

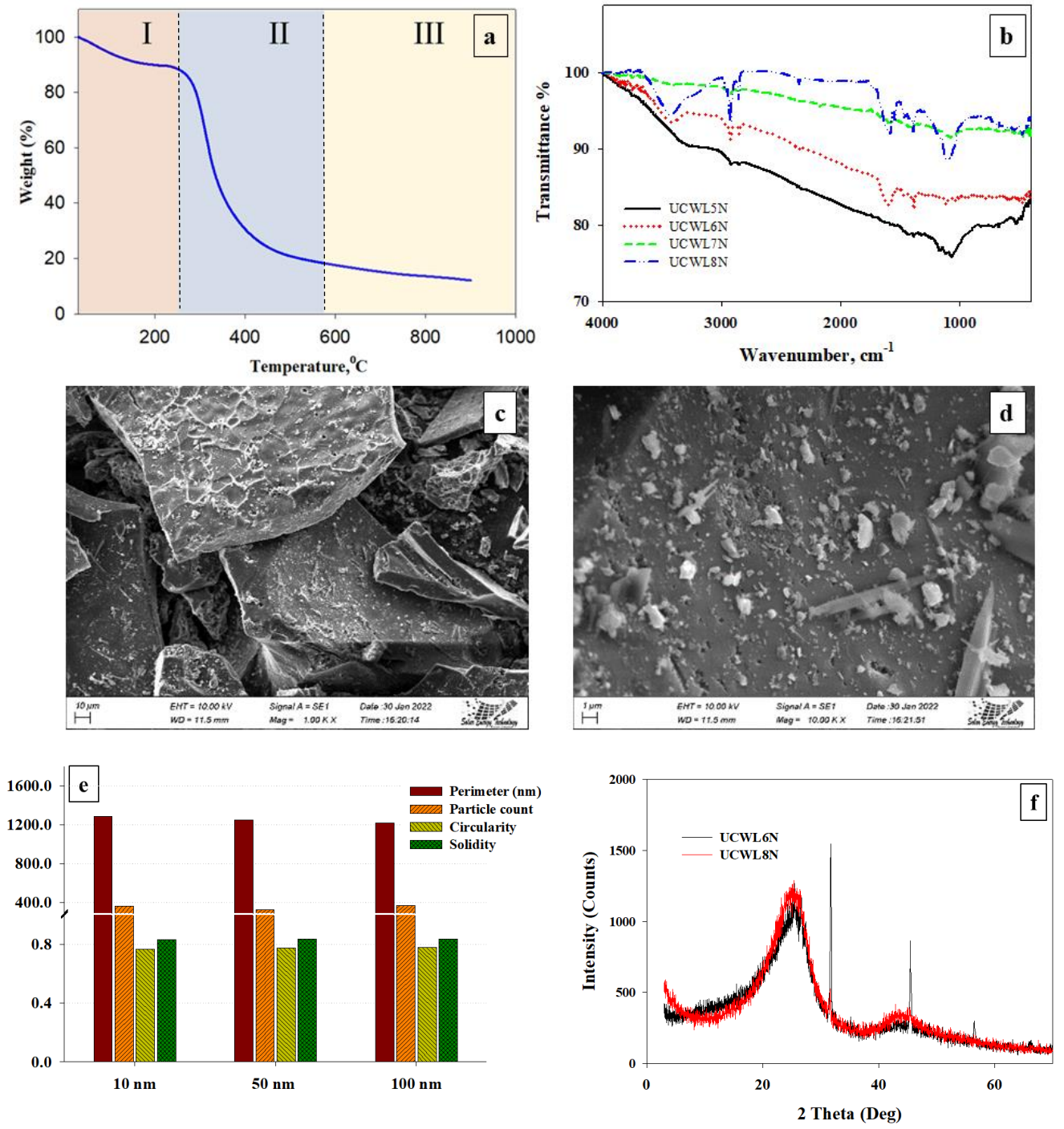

Fig. 1. (a) TGA analysis of WL in a N_2 atmosphere, **(b)** FT-IR spectra of UCWL5N, UCWL6N, and UCWL8N, (**c**, **d)** SEM images of UCWL6N, (**e**) different parameters obtained using ImageJ software for UCWL6N, and (**f**) XRD patterns of UCWL6N and UCWL8N.

The degree of crystallinity is additionally examined using the XRD technique. Fig. 1f depicts the XRD patterns of UCWL6N and UCWL8N. The diffraction patterns of all the samples exhibit two broad peaks with a distinct major peak at 2θ = ~26° and 44.3°. The peak at 2θ = ~26° is for (002) plane and the other peak and 2θ = 44.3° is for(100) plane. The broadness of the diffraction peaks indicates the presence of a significant quantity of disordered material and amorphous structures[12,29].

Electrochemical studies

The electrochemical behaviors of the materials prepared were investigated by cyclic voltammetric and GCD measurements. Fig. 2a represents the CVs recorded at different electrodes prepared and bare GC electrode.

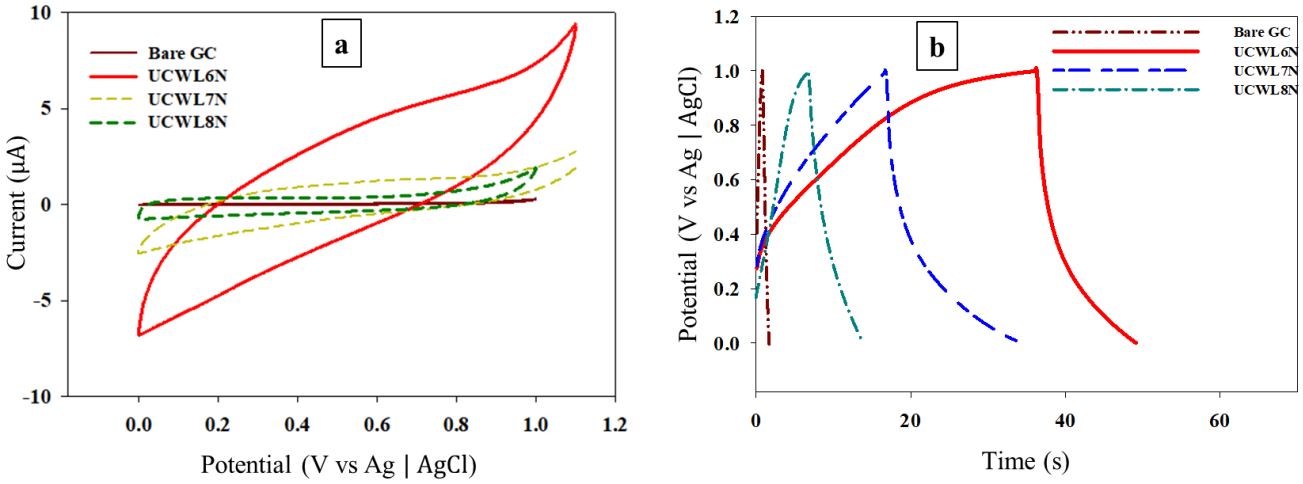

Fig. 2. (a) CVs recorded in 0.01 M NaCl solutions at υ of 10 mV s^{-1}, and (**b)** GCD responses of different electrodes measured at a current density of 0.1 A g^{-1}.

In general, the CVs of UCWL6N, UCWL7N, and UCWL8N demonstrate nearly a rectangular shape, indicative of EDL capacitance behavior[20-22,30,31]. While the characteristics of the CV measured with UCWL6N prepared at 600 °C are different from those of other electrodes, for example, the CV is relatively inclined with larger charging current. The analysis of these CVs indicate that all electrodes modified with carbon materials exhibited superior EDL capacitance (EDLC) compared to unmodified GC electrodes. The augmentation of calcination temperature results in a reduction of the EDLC. This may be ascribed to the enhancement in crystallinity that occurs at elevated temperatures[11-15].

Fig. 2b. depicts the charging-discharging behavior for the prepared electrodes. From the CV results, the potential range of GCD scans was chosen to be from 0 V to 1.0 V. The GCD responses indicate the lack of any Faradic reaction, which aligns with the findings obtained from prior CV measurements. Such an observation suggests that this electrode is ideally EDLC in character and has good ion adsorption-desorption behavior. The C_{sp} value was calculated from the GCD curve using Eq. (1), and UCWL6N showed the highest C_{sp} of 21 Fg^{-1} due to superior amorphous and porous structure.

CDI performance

As described above, UCWL6N offers the highest charge storage capacity among the electrodes studied. However, three materials studied were used to fabricate CDI electrodes using GC plate substrate as described in the experimental section. In order to envisage the advantages of using carbons derived from WL, the CDI performance of commercially available AC was also carried out.

Assembling and calibration of flow CDI system

The complete CDI setup with the dimension of the cell is depicted in Scheme 1. The homemade Teflon CDI flow cell consisted of slots for three pairs of electrodes arranged in parallel and separated by a Teflon spacer that allowed for water permeability, thereby mitigating the risk of short circuits. The width of the flow channel is 3.5 mm. The cell and effective electrode dimensions were 175 mm × 28 mm and 45 mm × 40 mm, respectively. The flow rate of the feed in the cell was controlled from 15 to 100 mL min^{-1} using a peristaltic pump. The calibrated optimum flow rate for the batch mode CDI system was 22-25 mL min^{-1}.

A DC power supplier applies a specific direct voltage and a conductivity meter monitors the change in conductivity of the feed solution. The calibrated optimum potential for the batch mode CDI system was 1.0-1.2 V. In the ion adsorption test cycle, a peristaltic pump propelled the feed solution through the channel of the CDI cell. The cell was then charged with a potential to facilitate the development of an EDL on the electrode surface, which led to the removal of ions from the solution. The process of eliminating ions was monitored through the continuous measurement of conductivity with a conductivity meter. In this study, NaCl removal efficiency was achieved using this CDI system for each electrode fabricated at identical operating conditions. This was carried out using 1.5 mM 125 mL of NaCl solution. The flow rate and potential were set at 23 mL min^{-1} and 1.0 V, respectively, and the electrodes are symmetric.

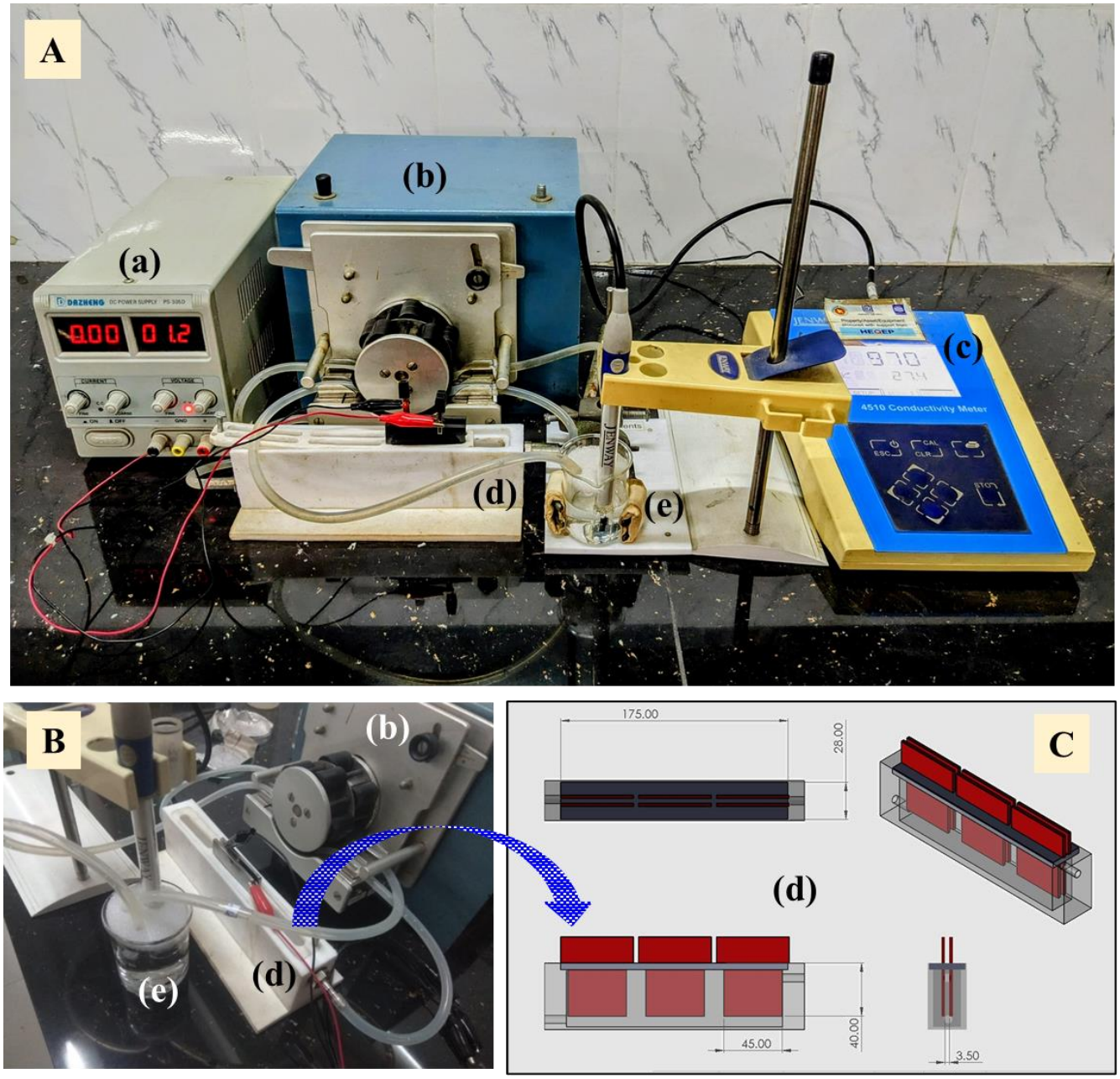

Scheme 1. Different components of the designed CDI system. (A) Photograph of assembled CDI system: (a) potentiostat, (b) peristaltic pump, (c) conductometer, (d) homemade electrochemical Teflon flow cell, and (e) solution reservoir containing conductometer cell, solution and silicon tubes connected to the flow cell. (B) Photograph of flow channel and CDI electrodes. (C) Schematic views of the flow channel designed.

Deionization measurements

Fig. 3 depicts the CDI performance of the developed UCWL electrodes. The profiles of change in conductivity, concentration, and removal efficiency of NaCl with time observed with UCWL6N and commercial AC are typically compared. The decrease in conductivity is indicative of removal of Na^+ and Cl^- ions from the solution. Due to the influence of the Coulombic forces of attraction, at the applied potential, the positively charged cations (i.e., Na^+) migrate towards the negatively charged electrode while the negatively charged anions (i.e., Cl^-) migrate towards the positively charged electrode. As a result, both cations and anions are adsorbed onto the surface of the electrodes, resulting in the observed decrease of solution conductivity.

From the results of conductivity, concentration of NaCl in solution, adsorption capacity, and removal efficiency were determined.

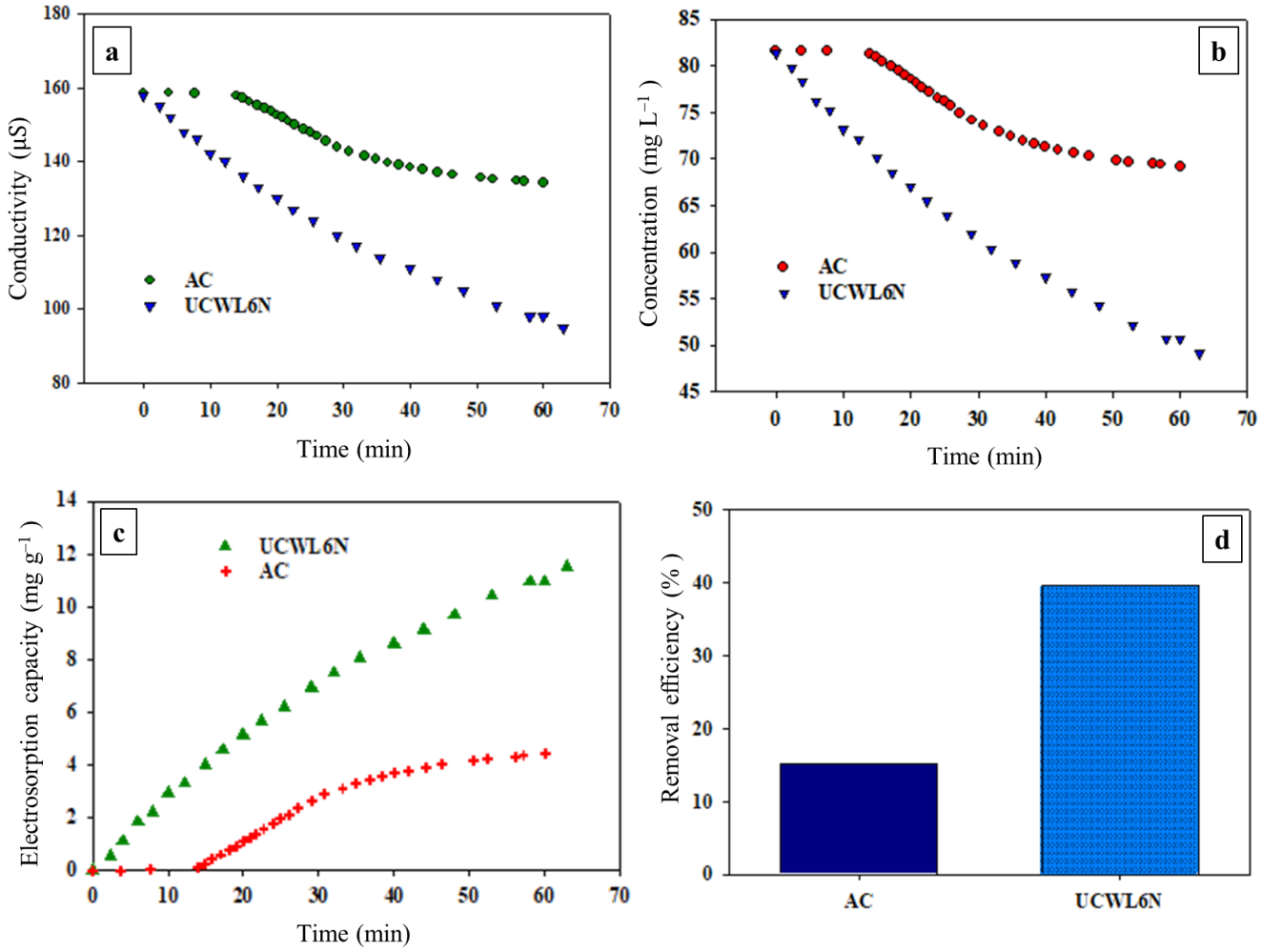

Fig. 3. Electrosorptive behavior of AC and UCWL6N electrodes in 1.5 mM 125 mL NaCl aqueous solution at 1.0 V potential. The flow rate of the solution was 23 mL min^{-1}. **(a)** Solution conductivity vs. time, **(b)** solution concentration vs. time, **(c)** electrosorption capacity vs. time, and **(d)** removal efficiency for UCWL6N and AC electrodes.

Fig. 3b illustrates the temporal changes in NaCl concentration. After a time span of 60-70 min, the state of adsorption equilibrium was attained, and prolonged period did not result in any change in the conductivity of the solution[23-27]. At this condition, the electrosorption capacity of the UCWL6N electrode was found to be superior to that of other electrodes developed, measuring 11.58 mgg^{-1}, whereas commercial AC is only 4.41 mgg^{-1}. UCWL7N and UCWL8N materials were also tested for the CDI performance. However, their electrosorption capacity was inadequate for detection by the conductivity meter. This was attributed to their low double layer capacitance that can be realized from the CV and GCD responses.

The superior electrochemical properties of the UCWL6N electrode, including improved charge-discharge cycles and higher electrical conductivity, account for its highest CDI performance among the synthesized electrodes[11,12]. The efficiency of removal was computed and subsequently presented in Fig. 3d. The AC electrode exhibited only 15% ion removal efficiency, while the UCWL6N electrode demonstrated a 40% efficiency. Thus, the UCWL6N demonstrates exceptional CDI performance among the materials studied and reported in literature, rendering it a viable option for employment in CDI applications aimed at desalination.

IV. Conclusions

This research reports the successful preparation of carbon material from readily available, cost-effective, eco-friendly precursor material derived from waste leather with reasonable yield, porous morphology, and efficient charge storage performance as well as the successful effort of assembling a flow system used for piloting CDI runs. The

impact of the activation temperature on the electrochemical and textural characteristics of porous electrodes were significant. The UCWL6N electrodes, prepared at 600 ^{o}C, have demonstrated favorable electrochemical performance and exhibit a high salt absorption capacity of 11.58 mgg^{-1} at 1.0 V, whereas commercial AC is only 4.41 mgg^{-1}. Although the study detailing the levels of N- and S-doping in carbon materials is underway, the observed high CDI performance of UCWL6N may be associated with amorphous, porous morphology of the materials under study. This study would be useful to develop low-cost materials for CDI electrode with enhanced efficiency.

Acknowledgment

The financial support of the Centennial Research Grant for the fiscal year 2020-2021 from the University of Dhaka is highly acknowledged.

References

1. Shiklomanov, I. A, 2000. Appraisal and assessment of world water resources.*Water International*, **25(1)**, 11-32.
2. Emmanuel, S. S., A. A. Adesibikan, and O. D. Saliu, 2023. Phytogenically bioengineered metal nanoarchitecture for degradation of refractory dye water pollutants: A pragmatic minireview. *Applied Organometallic Chemistry*, **37(2)**, 6946.
3. Mekonnen, M. M., and A. Y. Hoekstra, 2016. Four billion people facing severe water scarcity. *Science Advances*, **2(2)**, 1500323.
4. Subramani, A., and J. G. Jacangelo, 2015. Emerging desalination technologies for water treatment: A critical review. *Water Research*, **75**, 164-187.
5. Amiri, A., G. Ahmadi, M.Shanbedi, M. Savari, S. N. Kazi, and B. T. Chew, 2015. Microwave-assisted synthesis of highly-crumpled, few-layered graphene and nitrogen-doped graphene for use as high-performance electrodes in capacitive deionization. *Scientific Reports*, **5(1)**, 17503.
6. Cheng, Y., Z.Hao, C.Hao, Y. Deng, X. Li, K. Li, and Y. Zhao, 2019. A review of modification of carbon electrode material in capacitive deionization. *RSC Advances*, **9 (42)**, 24401-24419.
7. Zhang, S., Y. Wang, X. Han, Y. Cai, and S. Xu, 2018. Optimizing the fabrication of carbon nanotube electrode for effective capacitive deionization via electrophoretic deposition strategy. *Progress in Natural Science: Materials International*, **28(2)**, 251-257.
8. Suss, M. E., T. F. Baumann, W. L. Bourcier, C. M. Spadaccini, K. A. Rose, J. G. Santiago, and M. Stadermann, 2012. Capacitive desalination with flow-through electrodes. *Energy and Environmental Science*, **5(11)**, 9511-9519.
9. Sufiani, O., J. Elisadiki, R. L. Machunda, and Y. A. Jande, 2019. Modification strategies to enhance electrosorption performance of activated carbon electrodes for capacitive deionization applications. *Journal of Electroanalytical Chemistry*, **848**, 113328.
10. Lado, J. J., R. L. Zornitta, F. A. Calvi, M. Martins, M. A. Anderson, F. G. Nogueira, and L. A. Ruotolo, 2017. Enhanced capacitive deionization desalination provided by chemical activation of sugar cane bagasse fly ash electrodes. *Journal of Analytical and Applied Pyrolysis*, **126**, 143-153.
11. Elisadiki, J., T. E. Kibona, R. L. Machunda, M. W.Saleem, W. S. Kim, and Y. A. Jande, 2020. Biomass-based carbon electrode materials for capacitive deionization: a review. *Biomass Conversion and Biorefinery*, **10,** 1327-1356.
12. Dutta, S., S. Y. Huang, C. Chen, J. E. Chen, Z. A. Alothman, Y. Yamauchi, C. H. Hou, and K. C. W. Wu, 2016. Cellulose framework directed construction of hierarchically porous carbons offering high-performance capacitive deionization of brackish water. *ACS Sustainable Chemistry and Engineering*, **4(4)**, 1885-1893.
13. Zornitta, R. L., P. Srimuk, J. Lee, B. Krüner, M. Aslan, L. A. M. Ruotolo, and V. Presser, 2018. Charge and potential balancing for optimized capacitive deionization using lignin-derived, low-cost activated carbon electrodes. *ChemSusChem*, **11 (13)**, 2101-2113.
14. Silva, A. P., A. Argondizo, P. T. Juchen, and L. A. Ruotolo, 2021. Ultrafast capacitive deionization using rice husk activated carbon electrodes. *Separation and Purification Technology*, **271**, 118872.
15. Kim, M., M. D. Cerro, S. Hand, and R. D. Cusick, 2019. Enhancing capacitive deionization performance with charged structural polysaccharide electrode binders. *Water Research*, **148**, 388-397.
16. Liu, M., J. Niu, Z. Zhang, M. Dou, and F. Wang, 2018. Potassium compound-assistant synthesis of multi-heteroatom doped ultrathin porous carbon nanosheets for high performance supercapacitors. *Nano Energy*, **51**, 366-372.
17. Qian, K., A. Kumar, H. Zhang, D. Bellmer, and R. Huhnke, 2015. Recent advances in utilization of biochar. *Renewable and Sustainable Energy Reviews*, **42**,1055-1064.
18. Gautieri, A., S. Vesentini, A. Redaelli, and M. J. Buehler, 2011. Hierarchical structure and nanomechanics of collagen microfibrils from the atomistic scale up. *Nano Letters*, **11 (2)**, 757-766.
19. Konikkara, N., L. J. Kennedy, and J. J. Vijaya, 2016. Preparation and characterization of hierarchical porous carbons derived from solid leather waste for supercapacitor applications. *Journal of Hazardous Materials*, **318**, 173-185.
20. Hasan, M. A., M. A. Rahman, and M. M. Islam, 2023. Non-activated carbon for supercapacitor electrodes. *Biomass-Based Supercapacitors: Design, Fabrication and Sustainability*, 105-120.

21. Musa, A., M. M. Islam, M. A. B. H. Susan, and M. M. Islam, 2023. Polyoxometalate archetype-boosted stability and charge storage of 2D graphene nanosheets. *ECS Journal of Solid State Science and Technology*, 12,061005.

22. Hasan, M. A., M. M. Islam, M. A. B. H. Susan, and M. M. Islam, 2022. Supercapacitive behavior of manganese dioxide/tungsten bronze composites. *ECS Transactions*, **107(1)**, 12435.

23. Yan, C., L. Zou, and R. Short, 2014. Polyaniline-modified activated carbon electrodes for capacitive deionization. *Desalination*, **333(1)**, 101-106.

24. Yan, C., Y. W. Kanaththage, R. Short, C. T. Gibson, and L. Zou, 2014. Graphene/Polyanilinenanocomposite as electrode material for membrane capacitive deionization. *Desalination*, **344**, 274-279.

25. Liu, Y., C. Nie, X. Liu, X. Xu, Z. Sun, and L. Pan, 2015. Review on carbon-based composite materials for capacitive deionization. *RSC Advances*, **5(20)**, 15205-15225.

26. Lu, Ting, Y. Liu, X. Xu, L. Pan, A. A. Alothman, J. Shapter, Y. Wang, and Y. Yamauchi, 2021. Highly efficient water desalination by capacitive deionization on biomass-derived porous carbon nanoflakes. *Separation and Purification Technology*, **256**, 117771.

27. Liu, Y., X. Zhang, X. Gu, N. Wu, R. Zhang, Y. Shen, B. Zheng et al, 2020. One-step turning leather wastes into heteroatom doped carbon aerogel for performance enhanced capacitive deionization. *Microporous and Mesoporous Materials*, **303**, 110303.

28. Min, X., X. Hu, X. Li, H. Wang, and W. Yang, 2019. Synergistic effect of nitrogen, sulfur-codoping on porous carbon nanosheets as highly efficient electrodes for capacitive deionization. *Journal of Colloid and Interface Science*, **550**,147-158.

29. Mohamed khair, A. K., M. A. Aziz, S. S. Shah, M. N. Shaikh, A. K. Jamil, M. A. A. Qasem, I. A. Buliyaminu, and Z. H. Yamani, 2020. Effect of an activating agent on the physicochemical properties and supercapacitor performance of naturally nitrogen-enriched carbon derived from Albiziaprocera leaves. *Arabian Journal of Chemistry*, **13(7)**, 6161-6173.

30. Hasan, M. A., A. Musa, M. M. Islam, and M. M. Islam, 2023. Polyoxometalate archetypes as supercapacitor materials. *In Metal Phosphates and Phosphonates: Fundamental to Advanced Emerging Applications*, 267-281. Cham: Springer International Publishing.

31. Islam, M. M., M. Y. A. Mollah, M. A. B. H. Susan, and M. M. Islam, 2020. Frontier performance of in situ formed α-MnO_2 dispersed over functionalized multi-walled carbon nanotubes covalently anchored to a graphene oxide nanosheet framework as supercapacitor materials. *RSC Advances*, **10(73)**, 44884-44891.